the horizontally restrained toe on wall performance. Finally, each wall was carefully excavated in 300 mm deep layers while continuously monitoring strain gauges and extensometers attached to each instrumented reinforcement layer. In this way, the location of internal failure surfaces through the reinforced soil mass could be visually confirmed and stress relaxation in the reinforcement layers due to removal of overburden recorded.

Performance

A large amount of data has been gathered from the four test walls completed to date. Selected test results are reported here. A full report on the results of the long term test program is reserved for future publications.

Figure 5 shows the results of surveyed facing column profiles for Walls 1-3 at the end of construction. The dashed line in the figure is the target facing batter based on the geometry of the block units and the built-in concrete shear key location (i.e. this is the profile of the wall face if the blocks could be placed without backfill and each unit pushed forward against the shear key on the underlying block). The figure shows that the actual facing alignment is steeper than the target batter as a result of the incremental construction of the facing column. In addition, the amount of construction-induced rotational movement is greater for Walls 2 and 3 that were constructed with weaker reinforcement layers and a lesser number of reinforcement layers, respectively, compared to the control structure (Wall 1). The amount of construction-induced wall movement recorded at the crest of the facing column ranges from 2 to 4% of the height of the wall.

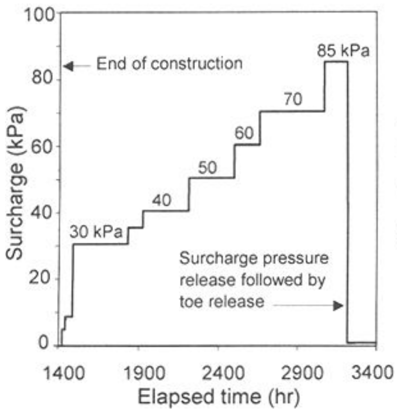

Figure 4. Surcharge history for Wall 2

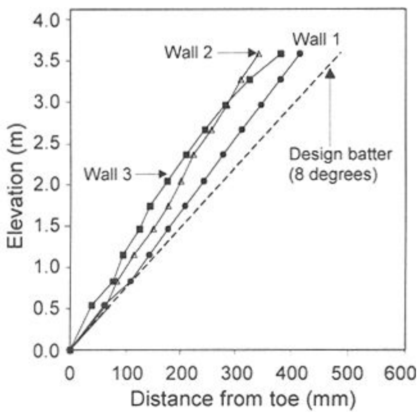

Figure 5. Facing column profiles at end of construction for Walls 1 to 3 (modular block facing)

This is a preview. Click here to purchase the full publication.

Figure 6 compares the surveyed facing profile of each of the four walls at end of construction plotted to a common datum. Not unexpectedly, the relatively more flexible wrapped-face wall can be seen to have displaced by about 250 mm at the base of the wall. This movement was generated largely at the time the bottom form work was removed after construction of the two lowermost layers of reinforcement. Nevertheless, the target batter of 8 degrees was reasonably well achieved for the remaining reinforcement layers.

Figure 7 illustrates wall deflections recorded for Wall 1. The horizontal deflections were recorded at reinforcement elevations on the outside of the facing column. Each jump in a deflection curve corresponds to the application of a new surcharge load. Creep of the structure is clearly evident in the figure as a result of the heavy surcharge loads applied to the backfill soil.

Figure 8 shows facing profiles for Wall 2 taken with respect to end of construction. Bulging of the facing column during surcharging is evident in the figure. The maximum outward movement of approximately 70 mm corresponds to about 2% of the height of the wall. The deflection profile for the wall shows a bulge at about ¾ of the height of the wall. At the end of the test the surcharge load was removed, the horizontal toe restraint released and the base of the wall allowed to move outward by about 20 mm. The outward movement of the toe clearly demonstrates that soil pressures acting on the back of the facing column were transmitted to the footing in this experiment.

Figure 9 shows the history of reinforcement displacements recorded by extensometers attached to layer 4 of Wall 2. The time-dependent deformation of the

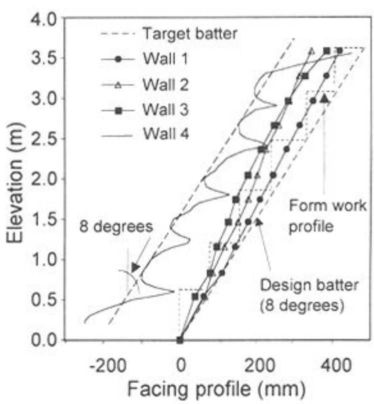

Figure 6. Facing profiles for Walls 1 to 4 at end of construction (from common datum)

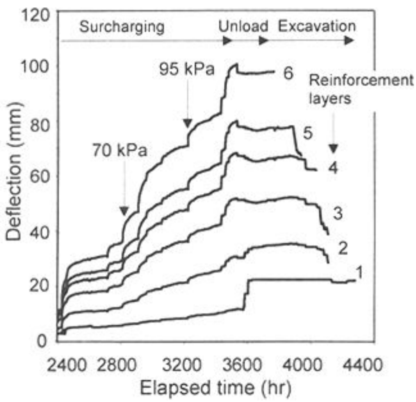

Figure 7. Horizontal deflections measured at face of Wall 1

This is a preview. Click here to purchase the full publication.

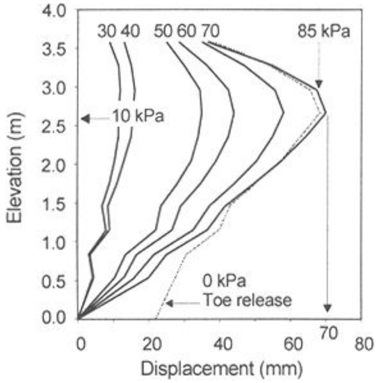

Figure 8. Facing profiles for Wall 2 taken with respect to end of construction

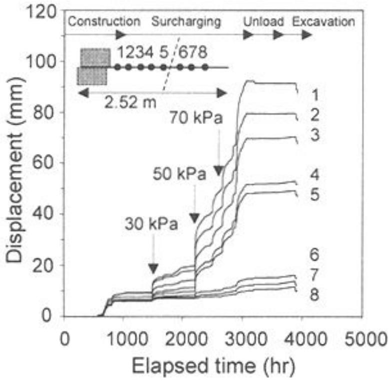

Figure 9. Extensometer displacements recorded for reinforcement layer 4 of Wall 2

reinforcement layer is clearly evident in the data. At the application of each surcharge load increment there was a corresponding jump in the extensometer movement followed by time-dependent deformations that increased in magnitude but at a decreasing rate until the application of the next load increment. As expected, the horizontal displacements in each reinforcement layer were largely irrecoverable after surcharge unloading. The plots in the figure also show that relatively small magnitudes of movement were recorded by the three extensometers located closest to the free end of the reinforcement layer. This behavior is consistent with the conventional notion that distinct active and anchorage soil zones develop at incipient collapse of a reinforced soil mass.

Figure 10 shows the distribution of strains in selected reinforcement layers at the end of construction of Wall 2. The plot shows that the strains are very low but that they are, nevertheless, largest at the connections. Figure 11 shows the distribution of strains in layer 5 of Wall 2 at different surcharge load levels. Only after the surcharge load reached 60 kPa did the peak reinforcement strain move from the connection to a location on the reinforcement corresponding to the internal failure plane in the reinforced soil zone.

Figure 12 shows the measured strain in the reinforcement at approximately the same elevation (layer 3) for Walls 1 to 4. At the end of construction (Figure 12a) the largest measured strains occurred close to the facing in all walls. The strains for Wall 4 were as great as four times the magnitude of the strains recorded for the comparable modular block structure (Wall 1) suggesting that the hard facing in combination with the restrained footing carries a significant portion of the lateral earth loads. The relatively high strains at the connections with respect to each

This is a preview. Click here to purchase the full publication.

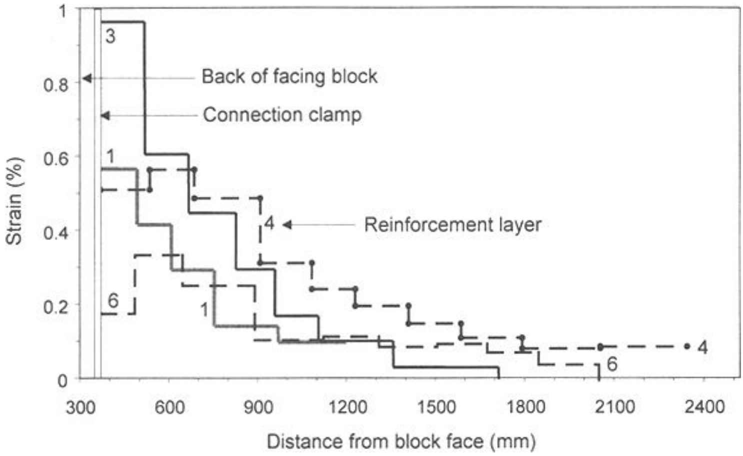

Figure 10. Distribution of strains at end of construction for Wall 2

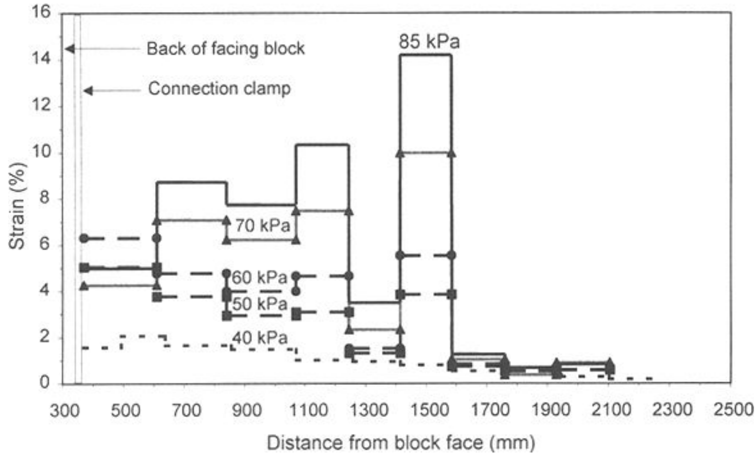

Figure 11. Strain in layer 5 for Wall 2 during surcharge loading

individual modular block wall can be attributed to the relative downward movement of the soil behind the facing. This movement occurs as a result of outward rotational movement of the facing column during construction (see Figure 5) and the settlement of the sand as a result of compaction during incremental construction. The high strains recorded at the same location in the wrapped-face wall are likely due to the downward sagging of the wrapped face (see Figure 6). A similar pattern of peak

This is a preview. Click here to purchase the full publication.

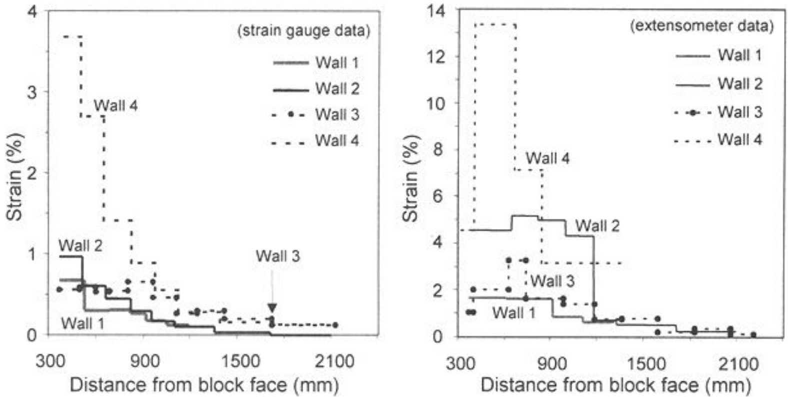

(a) End of construction (b) 60 kPa surcharge load

Figure 12. Measured strain in reinforcement layer 3 for Walls 1 to 4

strains close to the face has been reported by Bathurst et al. (1988) for a wrapped-face wall at end of construction. This earlier wall was constructed using a similar reinforcement material but with 750 mm reinforcement spacing and no artificial clamping of the reinforcement layers as described earlier.

At the end of construction, the strains for Wall 3 (four layers of reinforcement) were generally larger than for Wall 1 (6 layers of reinforcement) and were observed to propagate deeper into the reinforced soil zone. Similarly, the peak strains for Wall 2 (less stiff reinforcement) were larger than the strains recorded for Wall 1 constructed with reinforcement having twice the stiffness.

In Figure 12b the magnitude of strains are larger for each wall as a result of the 60 kPa surcharge load. The relative magnitudes of strain identified at end of construction are amplified in this figure with the exception noted earlier that peak strains for the modular block walls occur within the reinforced soil zone rather than at the connections. In the same figure it can be seen that a 50% reduction in the reinforcement stiffness resulted in a more than doubling of the measured strain (Wall 2 compared with Wall 1).

The co-incidence of the location of peak reinforcement strain in reinforcement layers for Wall 1 at peak surcharge load and the internal soil failure surface exposed at excavation is illustrated in Figure 13. The triangle-shaped markers on the figure denote the locations of directly measured peak changes in aperture length measured after reinforcement exhumation. These measurements corroborate the locations of peak strain recorded by strain gauges and inferred from extensometer readings. The failure plane was observed to exactly fit a log-spiral geometry using a plane strain

This is a preview. Click here to purchase the full publication.

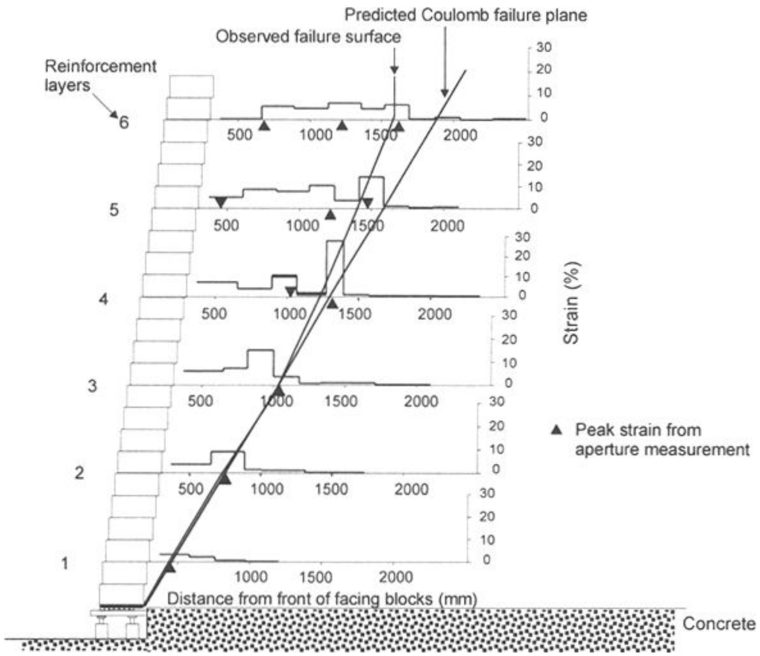

Figure 13. Location of peak reinforcement strain and internal failure surface for Wall 2

peak friction angle ϕ_{ps} = 44 °. However, from a practical point of view the predicted (and simpler) Coulomb failure plane using the same friction angle is reasonably accurate. A similar observation was made for Walls 2 and 3.

Figure 14 shows the history of horizontal toe load measurements recorded at the base of Wall 1 and the sum of connection loads recorded at each reinforcement layer. The figure shows that the restrained toe attracted a significant portion of the total horizontal earth force acting against the facing column. This is not surprising since the toe of the wall is very much stiffer than the reinforcement layers at end of construction. During surcharging, tensile load is mobilised in the reinforcement layers and proportionately more of the horizontal earth force exerted against the facing column is carried by the reinforcement layers. Nevertheless, the toe carries approximately 40% of the total horizontal earth force recorded at the facing column at the end of the surcharge loading program.

Figure 15 shows the history of vertical toe load forces recorded during construction of Wall 3. Each facing block was individually weighed and hence the self-weight of the facing column during construction can be plotted as the linear line

This is a preview. Click here to purchase the full publication.

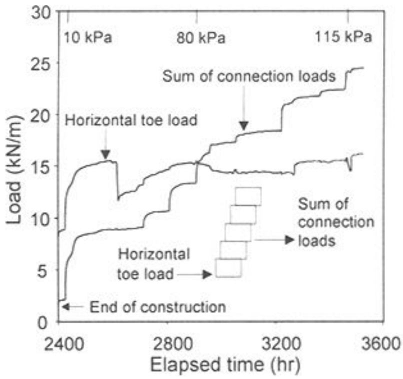

Figure 14. Horizontal toe load at the base of Wall 1 during surcharge loading

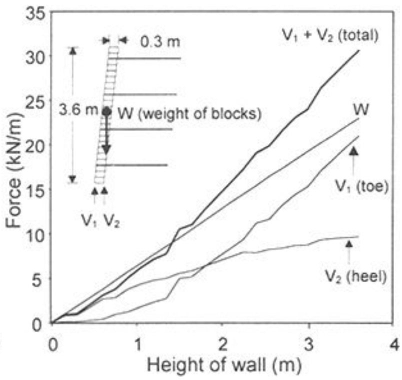

Figure 15. Vertical toe load forces for Wall 3 during construction

in the figure. Superimposed on the figure is the net vertical footing load and individual loads recorded by two parallel rows of load cells located at the toe and heel of the base plate directly below the facing column (see Figure 3). The sum of the vertical loads is greater than the self-weight of the facing column. This observation is attributed to the vertical downdrag force developed at the connections due to relative downward movement of the sand fill directly behind the facing column. This downward movement is a result of compaction of the soil and outward rotational movement of the facing column. While not shown here, the distribution of vertical earth pressures recorded by earth pressure cells located below the reinforced soil mass was also consistent with the development of vertical load transfer from the soil to the facing column (i.e. vertical earth pressures measured directly behind the facing column at the base of the soil mass were less than values predicted from soil self-weight and surcharge loading).

As the wall was built higher there was a shift of vertical load to the toe of the wall consistent with the notion of wall rotation about the toe of the facing column. However, the heel of each block unit was not unloaded indicating that the batter of the wall was sufficient to keep each block-to-block interface in compression. The hinge height (Simac et al. 1993; Bathurst et al. 1993) for this structure based on a target batter of 8 degrees is 2.1 m. An important implication of these measurements to design of the modular block structures in the current study is that the hinge height calculation is conservative for design.

Figure 16 shows the measured connection loads versus the predicted loads using Coulomb lateral earth pressure theory for the end-of-construction condition. In contrast to the triangular distribution of the predicted loads, the measured connection loads are almost uniform with depth. The magnitude and pattern of measured

This is a preview. Click here to purchase the full publication.

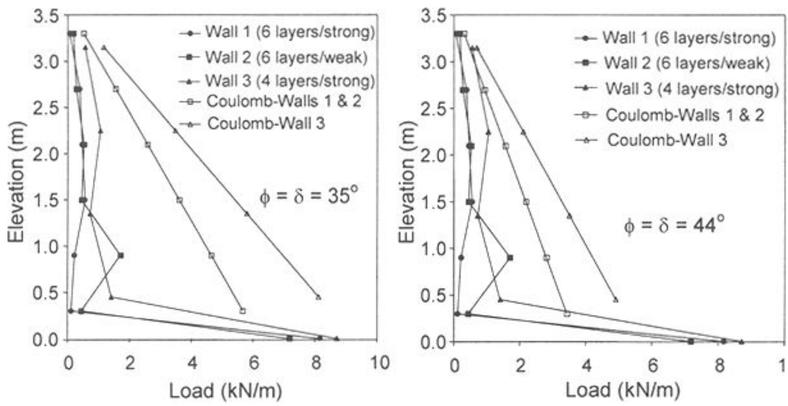

(a) Constant volume friction angle (b) Peak plane-strain friction angle

Figure 16. Measured versus predicted connection loads at the end of construction

connection loads is a direct consequence of the rigid toe attracting a significant portion of the horizontal earth forces acting on the facing column, the low stiffness of the geogrid reinforcement layers and, possible redistribution of reinforcement load during construction-induced outward movement of the facing column. Clearly, a shortcoming of conventional earth pressure theories applied to geosynthetic reinforced soil walls with a structural facing is their inability to account for the load that is carried by the restrained toe at the base of the facing column.

For the two reinforcement stiffness cases investigated, there was a negligible effect of reinforcement stiffness on magnitude of measured connection loads. There is a noticeable difference in connection load for Walls 1 and 2 at an elevation of 0.9 m that may be the result of local residual compaction stresses generated during the construction of Wall 2 (i.e. soil at this elevation may have been subjected to a higher degree of compaction). The larger reinforcement spacing used in Wall 3 results in a larger contributory facing area and hence larger predicted reinforcement load. This trend is confirmed by the measured loads shown in the figure.

Figure 16 also shows the influence of the magnitude of friction angle on predicted reinforcement loads. Figure 16a predictions are based on a constant volume friction angle, ϕ_{cv}, and Figure 16b shows predicted reinforcement loads using the peak plane strain friction angle, ϕ_{ps}. The selection of ϕ_{cv} produced an excessively conservative estimate of the reinforcement loads. Using the peak plane strain friction angle resulted in a conservative but more reasonable prediction of the connection loads particularly in the upper elevations of Walls 1 to 3.

This is a preview. Click here to purchase the full publication.

Conclusions

A large amount of data from the first four walls in this test program is currently being analysed and the results compared for the four different configurations. Some preliminary observations can be made:

- Connection loads for the structures with a modular block facing construction are the largest loads in the reinforcement at the end-of-construction condition.
- The toe of the wall in these experiments carried a significant portion of the horizontal earth forces acting on the hard facing column. This load capacity is not accounted for in current methods of analysis and design that use conventional earth pressure theories to predict reinforcement loads and hence is one source of conservatism in current design practice.
- The selection of the friction angle for the backfill material is another source of conservatism. Peak plane strain friction angles should be selected to reduce the conservatism in the analysis and design of geosynthetic reinforced soil structures constructed with a hard facing.
- A hard facing column is a structural element that acts to reduce the magnitude of strains that would otherwise develop in a wall with a flexible facing.
- The vertical normal load acting at the toe of the facing column is greater than the sum of the block weights due to soil down drag forces acting at the back of the facing column. This has important implications to connection design and confirms that for the wall batter used in these experiments the current NCMA method to calculate normal forces at the block interfaces is excessively safe.

Future Work

At the time of writing, six more reinforced soil walls are planned. These structures will isolate the influence of other material properties, geometry and facing type on the response of walls that are variations of Wall 1 (control) described in this paper. For example, walls will be constructed with polyester and steel mesh reinforcement materials, with different facing batters, smaller reinforcement spacing and with a full height propped panel configuration. Concurrently, the experimental results from this program and measurements from field-instrumented walls reported in the literature are being used to calibrate numerical models. In turn, numerical models will be used to extend the database of test configurations reported here to include higher walls, different soil types, different facing materials and a greater range of reinforcement spacing and properties.

Acknowledgements

Funding for the research program described here has been provided by the Washington State Department of Transportation, the AASHTO MSE Pooled Fund, the National Concrete Masonry Association, Natural Sciences and Engineering Research Council of Canada, Academic Research Program of the Department of

This is a preview. Click here to purchase the full publication.

National Defense (Canada) and grants from the Department of Infrastructure and Environment (DND Canada). The authors would like to acknowledge the contribution of Research Assistants (J. Escobar, M. Domingo, M. Leinhard, R. Madrigal and J. Lacharite) who helped to construct the walls described in the paper and Risi Stone Systems and Terrafix Inc. for provision of the facing units and reinforcement materials, respectively.

References

AASHTO 1996. Standard specifications for highway bridges. American Association of State Highway and Transportation Officials, Washington, D.C., USA.

Bathurst, R.J. 1990. Instrumentation of Geogrid-Reinforced Soil Walls, Transportation Research Board 1277, pp. 102-111.

Bathurst, R.J. 1991. Case Study of a Monitored Propped Panel Wall, Proceedings of the International Symposium on Geosynthetic-Reinforced Soil Retaining Walls, Denver Colorado, August 1991 (published by A.A. Balkema), pp. 159-166.

Bathurst, R.J. 1993. Investigation of Footing Restraint on Stability of Large-scale Reinforced Soil Wall Tests, 46'th Canadian Geotechnical Conference, Regina, Saskatchewan, pp. 389-398.

Bathurst, R.J. and Benjamin, D.J. 1990. Failure of a Geogrid-Reinforced Soil Wall, Transportation Research Board 1288, pp. 109-116.

Bathurst, R.J. and Simac, M.R. 1994. Geosynthetic Reinforced Segmental Retaining Wall Structures in North America, Invited keynote paper, 5th International Conference on Geotextiles, Geomembranes and Related Products, 6-9 September 1994, Singapore, Vol. 4, pp. 1275-1298.

Bathurst, R.J., Jarrett, P.M. and Lescoutre, S.R. 1988. An Instrumented Wrap-around Geogrid Wall, Proceedings of Third Canadian Symposium on Geosynthetics, Kitchener, Ontario, October 1988, pp. 71-78.

Bathurst, R.J., Simac, M.R. and Berg, R.R. 1993. Review of the NCMA Segmental Retaining Wall Design Manual for Geosynthetic-Reinforced Structures, Transportation Research Record, 1414, pp. 16-25.

Karpurapu, R.G. and Bathurst, R.J. 1995. Behaviour of Geosynthetic Reinforced Soil Retaining Walls using the Finite Element Method, Computers and Geotechnics, Vol. 17, No. 3, pp. 279-299.

McGown, A., Andrawes, K., Yeo, K. and Dubois, D. 1984. The Load-Strain-Time Behaviour of Tensar Geogrids, Symposium on Polymer Grid Reinforcement, Thomas Telford, London, UK, pp. 11-17.

Simac, M.R., Bathurst, R.J., Berg, R.R. and Lothspeich, S.E. 1993. National Concrete Masonry Association Segmental Retaining Wall Design Manual, National Masonry Concrete Association (NCMA), Herndon, Virginia, USA, March 1993, 250 p.

This is a preview. Click here to purchase the full publication.